

Photonuclear Activation by 20.5-Mev Gamma Rays*

W. E. DEL BIANCO AND W. E. STEPHENS

Department of Physics, University of Pennsylvania, Philadelphia, Pennsylvania

(Received December 12, 1961)

The photonuclear activation cross section of elements whose (γ, n) cross sections lead to a suitable positron activity has been measured using monochromatic gamma rays from the $T^3(p, \gamma)He^4$ reaction. The gamma rays were monitored by a 3-in. diam by 4-in. long sodium iodide crystal and calibrated with a $4\frac{1}{2} \times 6$ in. crystal whose response curve to the γ rays was determined. The absorption coefficient of these photons in NaI was determined by a good geometry transmission experiment. The positron activity was determined by a coincidence detector, consisting of two 5-in. diam by 2-in. long NaI crystals set on the annihilation radiation photopeaks. This detector was calibrated against a F^{18} positron source standardized in a 2π flow counter.

The $C^{12}(\gamma, n)C^{11}$ and $F^{19}(\gamma, n)F^{18}$ reactions were investigated over the range from 20.1 to 21.2 Mev. Structure, although reported by other experimenters, was not observed. The (γ, n) activation cross section was measured at 20.5 Mev for O^{16} , Cr^{50} , Fe^{54} , Cu^{63} , Zn^{64} , Mo^{92} , Sb^{121} , and Pr^{141} , giving cross section of 0.60 ± 0.12 , 29.1 ± 6.0 , 30.0 ± 4.8 , 52.5 ± 2.5 , 35.7 ± 1.8 , 35.4 ± 2.5 , 33.4 ± 2.7 , 51.7 ± 5.5 , respectively.

INTRODUCTION

MUCH of the recent photonuclear research has been made possible by the intensities of bremsstrahlung photons available from betatrons and synchrotrons. Nevertheless, the continuous nature of the energy distribution of these photons has made interpretation of results difficult. Furthermore, energy calibrations above 19 Mev are difficult because of lack of accurately known (γ, n) thresholds. Consequently, we are developing the use of monochromatic gamma rays, particularly the $T(p, \gamma)He^4$ gamma ray, to supplement and check the betatron measurements in the photon energy region above 20 Mev.

The present experiment, accomplished by the use of the monochromatic photons from the $T^3(p, \gamma)He^4$ reaction, was intended to improve the accuracy over the presently known cross-section values and to provide further information on the existence of fine structure in the giant resonance cross section. For various reasons that will be described further below, betatron cross-section values are often not in good agreement. A determination of the (γ, n) cross section by an independent method, using monochromatic gamma rays was, therefore, considered very useful. Since a photoactivation method was used and the resultant positron activity measured, the nuclei found suitable to investigate were: C^{12} , N^{14} , O^{16} , F^{19} , P^{31} , K^{39} , Cr^{50} , Fe^{54} , Cu^{63} , Ga^{69} , Br^{81} , Mo^{92} , Sb^{121} , Pr^{141} , and Ir^{191} . In this paper, the (γ, n) cross section is given at a photon energy $E_\gamma = 20.5$ Mev for C^{12} , O^{16} , F^{19} , Cr^{50} , Fe^{54} , Cu^{63} , Zn^{64} , Mo^{92} , Sb^{121} , and Pr^{141} . The other nuclides are presently to be measured.

Experiments with betatron "bremsstrahlung" have shown the existence of "breaks" in the activation curves of various light elements. These breaks have been explained in terms of energy levels in the target nuclei. Support for this hypothesis has come from the

study of the energy spectra of emitted photonucleons and from excitation curves of (γ, n) reactions.¹ Many of these experiments indicate the existence of this fine structure below and in the region of the giant resonance in some light nuclei. However, there are still discrepancies as to the number and properties of these levels.

In this laboratory, a monochromatic gamma-ray absorption experiment in C^{12} showed the presence of three energy levels in the range 20 to 21 Mev,² but an earlier activation measurement (presumably with the same energy resolution) failed to detect them.³ Re-measurement of the $C^{12}(\gamma, n)C^{11}$ cross section in the same energy range was therefore undertaken. It was decided to improve the reliability of the photon beam energy resolution and also to increase the accuracy of calibration both of the positron and photon detector to obtain good values for the cross sections.

EXPERIMENT

Protons from the University of Pennsylvania electrostatic accelerator were used to bombard a tritium target and produce monochromatic photons by the $T(p, \gamma)$ reaction. Proton energies from 500 kev to about 2 Mev with currents up to 50 μ a were obtainable. Measurement of the accelerator potential was obtained by using a "generating voltmeter" of the same type described by Trump.⁴ The linearity of the meter was originally checked by observing the resonances in the reaction $F^{19}(p, \alpha\gamma)O^{16}$ at 340.5 ± 0.2 kev at 872.5 ± 0.4 kev and by determining the threshold of the $H^3(p, n)He^3$ reaction at 1.0197 ± 0.0005 Mev.⁵ Because of the fact that the accel-

¹ W. E. Stephens, *Nuclear Spectroscopy*, edited by F. Ajzenberg-Selove (Academic Press, Inc., New York, 1960), Chap. IV; V. De Sabbata, Suppl. Nuovo cimento **II**, 225 (1959); E. G. Fuller and E. Hayward in *Nuclear Reactions*, edited by Endt, Demeur, and Smith (North-Holland Publishing Company, Amsterdam, 1961), Vol. II.

² E. E. Carroll and W. E. Stephens, Phys. Rev. **118**, 1256 (1960).

³ L. D. Cohen and W. E. Stephens, Phys. Rev. Letters **2**, 263 (1959).

⁴ J. G. Trump, F. J. Safford, and R. J. Van de Graaff, Rev. Sci. Instr. **11**, 54 (1940).

⁵ J. B. Marion, Revs. Modern Phys. **33**, 139 (1961).

* Supported by the joint program of the U. S. Atomic Energy Commission and the Office of Naval Research and by the National Science Foundation.

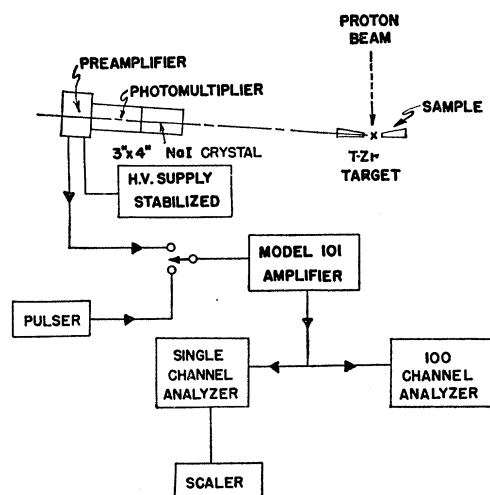


FIG. 1. General arrangement of target, sample, and monitor apparatus.

erator operates well at 1 Mv (terminal voltage), and since tritium targets were continuously used for this experiment, the energy calibration of the accelerator was periodically repeated using the $H^3(p,n)He^3$ reaction.

The energy of the tritium gamma rays as obtained from the conservation laws is

$$E_\gamma = \left(Q + E_p \frac{A-1}{A} \right) \left(1 - \frac{Q + E_p(A-1)/A}{2M_p A c^2} \right) \times \left(1 + \frac{\cos\theta}{A} \left(\frac{2E_p}{M_p c^2} \right)^{\frac{1}{2}} \right),$$

where $A-1$ and A are the mass numbers of T^3 and He^4 , respectively, and E_p and M_p , the kinetic energy and mass of the proton. The Q value is 19.812 ± 0.011 Mev.⁶ θ is the angle the photon direction makes with the incident proton beam, for a given proton energy. E_γ is a function of θ . Therefore, if a sample of finite dimensions is irradiated, the photons at various angles will have a variation in energy, which is usually referred to as "Doppler width."

The tritium targets consisted of tritium gas absorbed in zirconium metal, which had been evaporated onto a thin (10 mils) platinum or copper backing. The thickness of the target for 1.1-Mev protons was determined by measuring the $T(p,n)He^3$ neutron yield in the forward direction with a "long counter" as the proton energy was varied through the neutron threshold. The observed yield was compared with curves obtained by numerical integration of the thin targets results of Jarvis *et al.*⁷ for various assumed target thicknesses. The variation of target thickness with proton energy was obtained from Wahling's⁸ stopping power curves.

⁶ A. H. Wapstra, *Handbuch der Physik* (Springer-Verlag, Berlin, Germany, 1959), Vol. 38, p. 1.

⁷ G. A. Jarvis *et al.*, *Phys. Rev.* **79**, 932 (1950).

⁸ W. Wahling, *Handbuch der Physik* (Springer-Verlag, Berlin, Germany, 1958), Vol. 34, p. 193.

Targets of different thickness were used during the experiment. With fluorine and carbon samples, targets of 50-kev thickness were used in the range 20.1 to 20.7 Mev (photon energy), and in the range 20.7 to 21.1 Mev, targets 100-kev thick. With all the other samples the targets were about 250-kev thick.

In order to obtain a maximum photon flux and a minimum Doppler width, the samples were exposed to the photons around 90° in the form of annular rings surrounding the tritium target. The angle which the disk subtended to the source in the case of carbon and fluorine was made to give a Doppler width of 40 kev at 1-Mev proton energy. In all the other samples the angle was determined by choosing the maximum thickness of the samples to give a value approximately 0.25 for the absorption of the 0.5-Mev gamma rays. A 0.430-in. diam hole was drilled in the center of the disk to accommodate the tritium target. In the case of fluorine and carbon, the diameter of the samples was 5 in., equal to the diameter of the two sodium iodide crystals in the β^+ detector. For all the other samples the major radius was chosen so as to give 0.25 absorption of 20-Mev gamma rays. The carbon samples were made of reactor grade graphite with a purity of 99.93%. Fluorine was used in the form of "virgin" Teflon (polytetrafluoroethylene). The oxygen samples were obtained by pressing boric acid powder in a die and machining the resultant disk to the desired shape. All the other targets were made of pure metal (purity 99.9%).

A 3-in. diam by 4-in. long NaI crystal was used to monitor the 20-Mev gamma rays. It was placed with its front face at 24.65 in. from the tritium target, its axis forming an angle of $5^\circ 40'$ with the tritium target. The detected gamma-ray pulses were amplified and fed through a discriminator window which selected those pulses whose height fell between 16 and 22 Mev. The 20-Mev photon spectrum recorded with a Wilkinson-type multiple channel analyzer⁹ was used to determine the energy calibration of the discriminator window.

The over-all arrangement of the T-Zr target, the sample, and the photon monitor are shown in Fig. 1. The sample to be irradiated and the crystal lie above the 90° plane to eliminate the complication of using photons which had passed through the platinum or copper backing. Because of this arrangement, the energy distribution for photons passing through the sample can be approximated with a trapezoid whose area represents the total number of gamma rays that bombard the target nuclei; its base has a length equal to the sum of the Doppler width, ΔE_D , and three quarters of the proton target thickness ΔE_t ; its upper edge has a length equal to the absolute value of the difference of ΔE_t and ΔE_D . The photon energy resolution, defined as the full-width at half-maximum of the

⁹ D. H. Wilkinson, *Proc. Cambridge Phil. Soc.* **46**, 508 (1949).

energy distribution, is then equal to ΔE_t or ΔE_D , whichever is larger.

The samples were irradiated for a convenient length of time, equal to a multiple or submultiple of the half-life T . They were then transported to the detection apparatus in 50 sec and counted in the positron detector for a preset time, also of the order of the half-life. The positron detector consisted of two NaI(Tl) crystals 5 in. in diameter by 2 in. thick placed $\frac{1}{2}$ -in. apart. The pulses from the two crystals were amplified, channeled between 380 and 600 kev, and put into coincidence (resolving time $\approx 2 \mu\text{sec}$). This arrangement, with an 18-in. iron and lead shield around it, had a background of 3 counts/min.

ABSOLUTE CALIBRATION OF PHOTON MONITOR AND POSITRON DETECTOR

A. Photon Monitor

Because of the lack of experimental data on the absorption coefficient of NaI in the 20-Mev gamma energy range, and since theoretical calculations are subject to uncertainties for pair production and photonuclear absorption, the absorption coefficient of NaI was measured experimentally. A 3-in. diam by 4-in. long sodium iodide crystal was used as absorber in a good geometry transmission-type measurement.¹⁰ A lead collimator, consisting of a 4-in. thick lead block with a tapered hole through its center, was placed between the absorbed crystal and the detector. A 0.5-in. thick graphite disk was placed over the face of the detector crystal to reduce the correction for Compton scattered electrons and pair electrons which originated in the back end of the absorber. The detector was a 4.5-in. diam by 6-in. long NaI(Tl) crystal and a 3-in. diam by 4-in. long NaI(Tl) crystal was used to monitor the gamma-ray intensity. The absorption coefficient, when corrected for in-scattered Compton photons, Compton electrons, and pair electrons from the lead collimator, was found to be equal to $0.166 \pm 0.003 \text{ cm}^{-1}$. The value for the total cross section obtained is $11.6 \pm 0.21 \text{ b}$ using a density of 3.67 g/cm^3 . The value calculated theoretically is 11.10 b in good agreement with the value observed. The calculated contributions to the theoretical cross section of the various processes are shown in Table I.

TABLE I. Theoretical cross sections at 20.48 Mev.

Process	$\sigma \times 10^{24} \text{ (cm}^2\text{)}$
Compton	1.908
Pair production	8.86
Triplet production	0.16
Nuclear photoeffect	0.14
Atomic photoelectric effect	0.03

¹⁰ W. E. Del Bianco, H. Staub, W. E. Stephens, and G. Tessler. Paper 22, in "Proceedings of the Total Absorption Gamma-Ray Spectroscopy Symposium," Gatlinburg, Tennessee, May 10-11, 1960, TID-7594, Office of Technical Services, Dept. of Commerce, Washington, D. C.

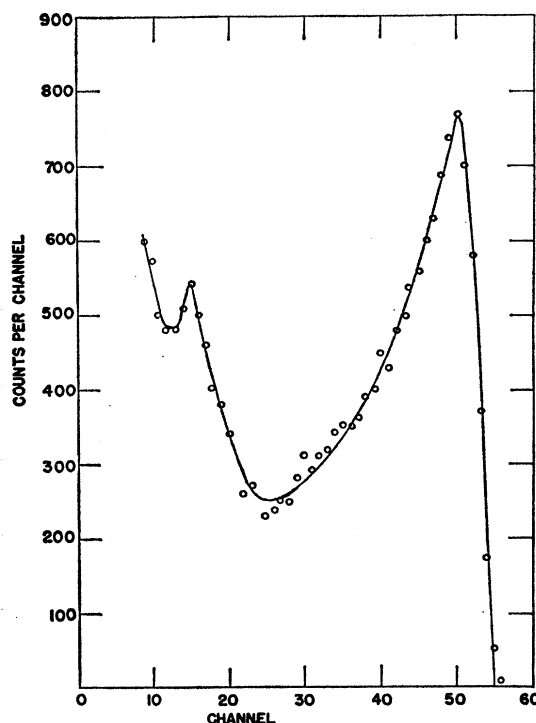


FIG. 2. Spectrum of the 20.5-Mev gamma rays in a 3×4 in. NaI crystal.

Because of background in the lower energy region, the complete shape of the 20-Mev photon spectrum could not be well determined in the 3-in. by 4-in. sodium iodide crystal (Fig. 2). The gamma-ray intensity was calibrated by a larger crystal, 4.5-in. diam by 6-in. long, which was placed with its front face at 25.6 in. from the target and collimated with a lead block (4-in. thick) having a tapered hole through its center that projected a circle of 1-in. diam on the front face of the crystal. For such an arrangement the shape of the 20-Mev photon spectrum can be more easily evaluated at low energies (less than 10 Mev) and can be approximately represented with a straight line passing through the origin (Fig. 3). The validity of this extrapolation has been tested in an experiment recently performed in this laboratory, where the energy which had escaped from the crystal proper was detected by another crystal in a coincidence arrangement. The results of this measurement which will appear in a separate article are consistent with the calculations and measurements of Kockum and Starfelt.¹¹ We believe the uncertainty in the calibration of the gamma-ray monitor, so obtained, to be less than $\pm 3.5\%$.

B. Positron Detector

The absolute efficiency of the annihilation radiation detector is a function of the radial position r of the positron source in the gap and the self-absorption in

¹¹ J. Kockum and N. Starfelt, Nuclear Instr. 4, 171 (1959).

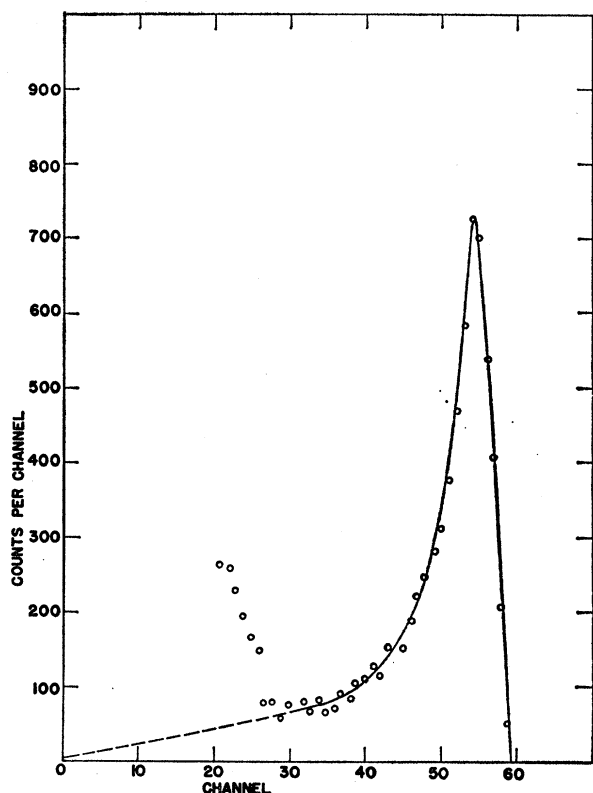


FIG. 3. Spectrum of the collimated 20.5-Mev gamma rays in a 4.5×6 in. NaI crystal.

the sample. Measurements showed that the detection efficiency η did not depend on the azimuthal angle, nor on the axial position in the gap. In order to find the effect of self-absorption and variation in r , η was measured for each target as a function of the radius, using F^{18} positrons counted in a 2π proportional counter. The F^{18} source was obtained by bombarding Teflon disks with the bremsstrahlung beam of the University of Pennsylvania betatron. The maximum energy of the photon beam was kept below the threshold value of the reaction $C^{12}(\gamma, n)C^{11}$ at 18.7 Mev. The half-life of F^{18} was measured both with the positron detector and the 2π proportional counter. The activity was recorded over a period of a few half-lives. The two values were found to be in agreement and they yielded $T = (108.3 \pm 1.0)$ min. The observed activity of the β^+ source in the proportional counter had to be corrected for self-absorption in the source and for backscattering from the source holder. Roalsvig and Haslam¹² have given an empirical formula to correct for these two factors, which is valid in the range of maximum electron energies from 0.84 to 3.44 Mev. The maximum energy of F^{18} positrons is only 0.65 Mev, which is outside Roalsvig and Haslam's experimental range; therefore, the correction factors for F^{18} self-absorption

¹² J. P. Roalsvig and R. N. H. Haslam, Can. J. Phys. 37, 499 (1959).

in Teflon were determined directly, following a similar experimental procedure, and were found to be consistent with the extrapolation of Roalsvig and Haslam results within the experimental errors.

Figures 4 and 5 illustrate the behavior of η as a function of r for carbon and zinc samples. The curves for the Teflon and boric acid samples are similar to those of Fig. 4; for all the other samples the radial dependence of the absolute efficiency follows very closely that of zinc.

The absolute efficiency at the center of the β^+ detector was found to be $\eta_0 = 0.195 \pm 0.006$. The error is attributed mainly to counting statistics (1 to 3%), and to the extrapolation procedure required in the Roalsvig-Haslam method.

RESULTS

The cross-section $\sigma(\gamma, n)$ can be written for this experimental arrangement as

$$\sigma(\gamma, n) = R a f (1/\epsilon F N) (\epsilon \gamma \alpha / \delta), \quad (2)$$

where R is the ratio between the number of positrons detected in the β^+ detector in the counting time t_c and the number of photons recorded by the gamma-ray monitor in the activation time t_a ; a is the ratio of t_a to the half-life T ; f is the 20-Mev gamma ray transmission

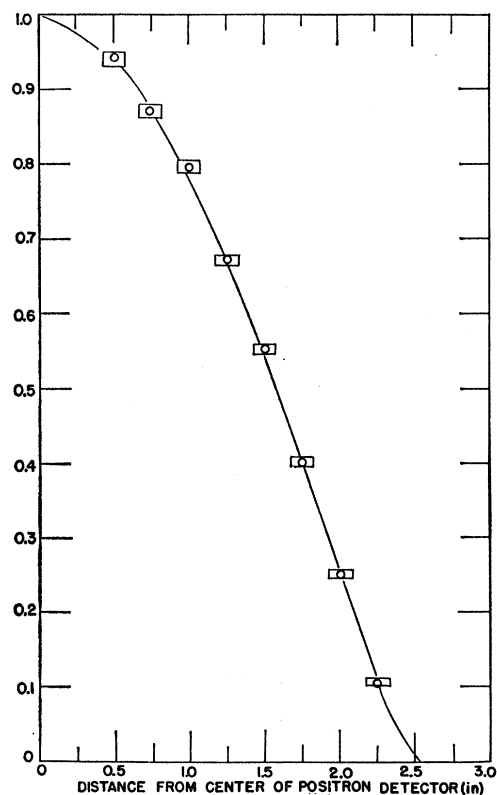


FIG. 4. Relative efficiency of the positron detector as a function of radial position for a carbon sample.

through the sample; ϵ is the fraction of disintegrations which occur by positron emission; F is equal to $1.443(1 - e^{-\lambda t_a})(1 - 2^{-\lambda t_a})e^{-\lambda t_w}$, where t_w is the time elapsed from the end of an irradiation to the beginning of the activation counting; N is the number of nuclei of the specific isotope contained in the unit volume of the sample; ϵ_γ is the efficiency of the photon monitor, and α the ratio of the solid angle subtended by the crystal to the solid angle subtended by the sample at the tritium target; δ is the effective efficiency of the β^+ detector for a particular sample. In the evaluation of the cross section for the various nuclei, the half-life T , the isotopic percentage Z , and the electron capture coefficient $(1 - \epsilon)$ were taken from the tables of Strominger *et al.*¹³ From the same source were also taken the decay schemes of the active nuclei. For Fe^{53} , Zn^{63} , Cr^{49} , Sb^{120} , the decay schemes were assumed to be as given in references 14–17, respectively.

A. (γ, n) Cross Sections at 20.48 Mev

The values for the (γ, n) cross sections at 20.48 Mev are recorded in Table II. The uncertainty associated with the cross-section value represents the standard error due to counting statistics and other Gaussian errors, but does not include the error involved in the determination of the absolute efficiency of the positron and photon detectors.

The mean energy of the photon beam was calculated to be 20.48 Mev, and at this energy the Doppler width for all the samples was approximately 40 keV. The target thickness was measured to be about 250 keV. Therefore, the gamma-ray energy resolution was 250 keV.

C^{11} , O^{15} , F^{18} , Cu^{62} , and Pr^{141} are known to decay directly to the ground state of the daughter nuclei either by positron emission or electron capture. The decay schemes of Cr^{49} , Fe^{54} , Zn^{63} , Mo^{91} , and Sb^{120} are

TABLE II. Photonuclear cross sections at 20.48 Mev.

Nucleus	$\sigma(\gamma, n)$ (in barns)
C^{12}	1.04 ± 0.11
O^{16}	0.60 ± 0.12
F^{19}	3.30 ± 0.41
Cr^{50}	29.1 ± 6.0
Fe^{54}	30.0 ± 4.8
Cu^{63}	52.5 ± 2.1
Zn^{64}	35.7 ± 1.7
Mo^{92}	35.4 ± 2.3 (ground state)
Sb^{121}	33.4 ± 2.5 (ground state)
Pr^{141}	51.7 ± 5.4

¹³ D. Strominger, J. M. Hollander, and G. T. Seaborg, *Revs. Modern Phys.* **30**, 585 (1958).

¹⁴ R. H. Nussbaum, R. van Lieshout, and A. H. Wapstra, *Phys. Rev.* **92**, 207 (1953).

¹⁵ O. Huber, H. Medicus, P. Preiswerk, and R. Steffen, *Helv. Phys. Acta* **20**, 495 (1947).

¹⁶ R. H. Nussbaum, A. H. Wapstra, G. H. Nijgh, L. M. Ornstein, and N. F. Verster, *Physica* **20**, 165 (1954).

¹⁷ C. L. McGinnis, *Phys. Rev.* **109**, 888 (1958).

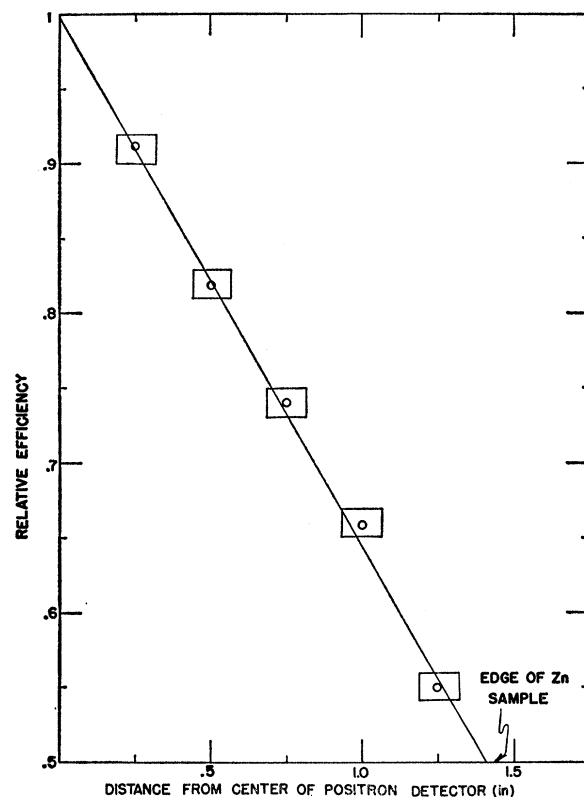


FIG. 5. Relative efficiency of the positron detector as a function of radial position for a zinc sample.

of a more complex type. In the case of Cr^{49} , Fe^{53} , and Zn^{63} , the resultant nucleus, following β^+ decay or electron capture, may be left in an excited state, from which decay occurs immediately by gamma emission. If the positron annihilation gamma rays interact with the two crystals so as to give pulses in the 0.5-Mev peak in each, and at the same time the excited state gamma ray produces a pulse in either crystal it will knock one of the two 0.5-Mev pulses out of the discriminator window, and the positron will not be detected. A correction had, therefore, to be calculated for all cases which involved transitions to excited states. The (γ, n) cross section had to be increased by 37% in Cr^{50} , by 20% in Fe^{54} , and by 2% in Zn^{64} .

For Sb^{120} there exists a metastable state above the ground state.¹⁷ Since the threshold of the reaction $\text{Sb}^{121}(\gamma, n)\text{Sb}^{120}$ occurs at 9.3 Mev, 20.5-Mev gamma rays can produce Sb^{120} in both the lower and higher energy levels. The two levels decay independently and without mixing to states in Sn^{120} with different half-lives: $T_m = 5.8$ days and $T_g = 16$ min. Due to the length of the 5.8-day half-life, it was not practical to observe this decay; consequently, the value tabulated in Table II represents the cross section of the reaction $\text{Sb}^{121}(\gamma, n)\text{Sb}^{120}$ leaving Sb^{120} in the ground state only.

In the case of Mo^{91} , there exists a metastable state¹⁸

¹⁸ F. B. Smith, N. B. Gore, R. W. Henry, and R. A. Becker, *Phys. Rev.* **104**, 706 (1956).

with a half-life (66 sec) short compared to the half-life of the ground state (16 min), which decays partially by gamma emission to the ground state of Mo^{91} (branching ratio 57%) and partially by positron emission or electron capture to the daughter nucleus Nb^{91} . The cross section for the (γ, n) process leaving Mo^{91} in the ground state was obtained, using the ratio of the two cross sections to the ground and to the metastable state as given by Katz and co-workers¹⁹ after proper correction for an erroneous decay scheme.

B. Carbon and Fluorine Activation

Carbon and fluorine activation curves are plotted in Figs. 6 and 7. The flags on each point represent the counting statistics. The energy resolution varied from 55 keV at 20.1 MeV to 45 MeV at 20.4, to 50 keV at 20.7 MeV, then to 65 keV from 20.7 MeV.

In the case of fluorine, a Teflon sample had to be used, and the C^{11} activity had, therefore, to be subtracted from the activity actually detected. The threshold of the reaction $\text{F}^{19}(\gamma, n)$ occurs at 20 MeV and the cross section, according to Horsley,²⁰ rises almost linearly up to 21 MeV, where its value is about 0.15 mb. At 20.5-MeV energy the contribution to the number of positrons detected in our experiment is estimated to be only 0.1% and was therefore neglected.

DISCUSSION

A. Absolute (γ, n) Cross Sections

$\text{Cu}^{63}(\gamma, n)\text{Cu}^{62}$ (reference 21)

The decay scheme of Cu^{63} was assumed simple; a value zero was assumed for the electron capture coefficient and all the transitions were assumed to occur through positron emission to the ground state of Ni^{62} . However, there is some suggestion of a possible few percent electron capture decay to the ground state and possibly to the excited states. Berman estimates a minimum theoretical value for the electron capture coefficient equal to 2%. With this uncertainty the $\text{Cu}^{63}(\gamma, n)\text{Cu}^{62}$ cross section at 20.5 MeV is determined to be 52.5 ± 2.5 mb. This agrees with the betatron results of Diven (45 mb), Byerly (50 mb), Katz (45 mb) (reduced from the quoted 50 mb for revised calibration), and Khron (45 mb). However, the electron beam measurements of Berman and Brown (32 mb), and of Scott and Hanson (14 mb), are appreciably off. In the case of Berman and Brown, this may be due to the distortion of the giant resonance by the use of large

energy increments. In the case of Scott and Hanson, incorrect activity calibration may have lowered the cross section.

$\text{C}^{12}(\gamma, n)\text{C}^{11}$ (reference 22)

The sharply rising character of the cross-section curve for this reaction near 20.5 MeV imposes a severe test on the energy calibration of the betatron work. The curves of Katz and Carver come closest to ours. However, a shift in energy of less than 1 MeV would allow all the betatron results to fall onto our fragment of the cross-section curve. While there may be intensity calibration errors in addition, they are not uniquely revealed in this comparison. The only other gamma-ray work, that done by Day with 200- to 450-kV resolution, does not quite overlap our energy range, but seems consistent with our results.

The electron beam measurement of Barber may have again been slightly distorted by the use of a large energy increment, which may have widened the narrow giant resonance enough to account for his difference with our results.

$\text{O}^{16}(\gamma, n)\text{O}^{15}$ (reference 23)

Here again, the 20.5-MeV point is at the foot of the giant resonance and possibly in the region of fine structure. Consequently, the difference between the values determined by betatron measurements and our results may easily be ascribed to incorrect energy calibration and lack of resolution of structure or both. The work of Spicer indicates a dip in the cross-section curve near 20.5 MeV.

$\text{F}^{19}(\gamma, n)\text{F}^{18}$ (reference 24)

In fluorine the 20.5-MeV photon energy is in the region of the maximum of a rather flat giant resonance. Here energy calibration probably does not account for the differences between the betatron results and our value. Horsley's result (3.5 mb) agrees quite well with our value of 3.3 ± 0.43 mb. Ferguson's value (8.5 mb) is based on the calibration of neutron detectors and seems too large, probably due to calibration errors.

²² $\text{C}^{12}(\gamma, n)\text{C}^{11}$ reaction. G. C. Baldwin and G. S. Klaiber, Phys. Rev. **73**, 1156 (1948); L. Katz and A. G. W. Cameron, Can. J. Phys. **29**, 518 (1951); L. W. Jones and K. M. Terwilliger, Phys. Rev. **91**, 699 (1953); R. Nathans and J. Halpern, Phys. Rev. **93**, 437 (1954); W. C. Barber, W. D. George, and D. D. Reagan, Phys. Rev. **98**, 73 (1955); J. A. Carver and K. H. Lokan, Australian J. Phys. **10**, 312 (1957); B. C. Cook, Phys. Rev. **106**, 300 (1957).

²³ $\text{O}^{16}(\gamma, n)\text{O}^{15}$ reaction. H. E. Johns, R. J. Horsley, R. N. H. Haslam, and A. Quinton, Phys. Rev. **84**, 856 (1951); R. Montalbetti and L. Katz, Can. J. Phys. **31**, 798 (1953); G. A. Ferguson, J. Halpern, R. Nathans, and P. F. Yergin, Phys. Rev. **95**, 776 (1954); J. H. Carver and K. H. Lokan, Australian J. Phys. **10**, 312 (1957); B. M. Spicer, Australian J. Phys. **10**, 326 (1957).

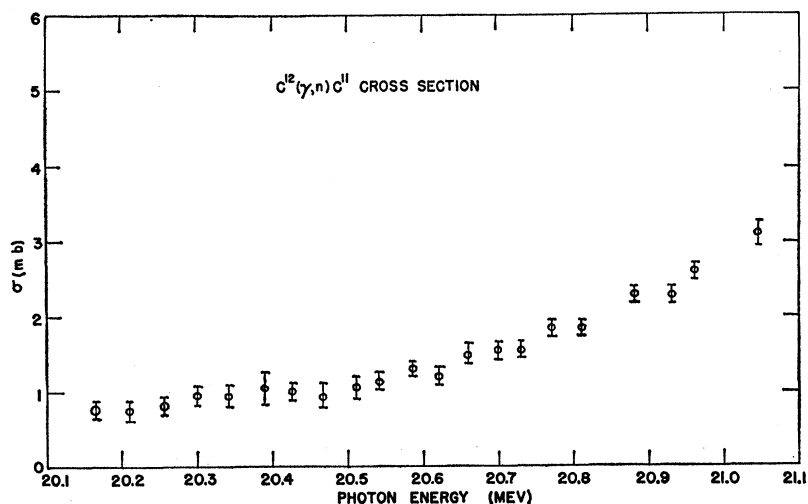
²⁴ $\text{F}^{19}(\gamma, n)\text{F}^{18}$ reaction. R. J. Horsley, R. N. H. Haslam, and H. E. Jones, Phys. Rev. **87**, 756 (1952); G. A. Ferguson, J. Halpern, R. Nathans, and P. F. Yergin, Phys. Rev. **95**, 776 (1954); J. G. V. Taylor, L. B. Robinson, and R. N. H. Haslam, Can. J. Phys. **32**, 238 (1954).

¹⁹ L. Katz, R. G. Baker, and R. Montalbetti, Can. J. Phys. **31**, 250 (1953).

²⁰ R. J. Horsley, R. N. H. Haslam, and H. E. Jones, Phys. Rev. **87**, 756 (1952).

²¹ $\text{Cu}^{63}(\gamma, n)\text{Cu}^{62}$ reaction. B. C. Diven and G. M. Almy, Phys. Rev. **80**, 407 (1950); L. Katz and A. G. W. Cameron, Can. J. Phys. **29**, 518 (1951); P. R. Byerly, Jr. and W. E. Stephens, Phys. Rev. **83**, 54 (1951); V. E. Krohn, Jr. and E. F. Schrader, Phys. Rev. **87**, 685 (1952); A. I. Berman and K. L. Brown, Phys. Rev. **96**, 83 (1954); M. B. Scott, A. O. Hanson, and D. W. Kerst, Phys. Rev. **100**, 209 (1955).

FIG. 6. The $C^{12}(\gamma,n)C^{11}$ reaction cross section in millibarns as a function of photon energy in Mev.



$Cr^{50}(\gamma,n)Cr^{49}$ (reference 25)

It is to be noted that the decay scheme of Cr^{49} is rather complex, and perhaps not too well known. In this experiment, the decay scheme given by Nussbaum¹⁶ was used. The branching ratios to the ground, first, and second excited states were taken equal to 0.52, 0.13, and 0.28, respectively. Since the sum of the branching ratios is 0.93, we assumed that the residual 7% of decays proceed through electron capture. The measurements of Goldenberg and Katz based on ionization chamber calibration and activation detection of positrons with a thin wall counter are in good agreement with our value.

$Fe^{54}(\gamma,n)Fe^{53}$ (reference 26)

Katz's theoretical value of 0.03 for the electron capture coefficient was used in our calculations together with the decay scheme proposed by Nussbaum.¹⁴ As a consequence of the positron decay of Fe^{53} to the 0.370-Mev excited state of Mn^{53} , the cross section, calculated from the number of positrons actually detected, had to be increased by 20%.

The resulting cross section (30 mb) is smaller than Katz's (1951) 55 mb, and in agreement with Carver's (1957) 32 mb. Both Katz and Carver detected the reaction by the resultant positron activity.

$Zn^{64}(\gamma,n)Zn^{63}$ (reference 27)

The cross section of the reaction $Zn^{64}(\gamma,n)Zn^{63}$ has been measured by Katz and co-workers (1951). They used the same experimental arrangement as for Fe^{54}

²⁵ $Cr^{50}(\gamma,n)Cr^{49}$ reaction. J. Goldenberg and L. Katz, Can. J. Phys. **32**, 49 (1954).

²⁶ $Fe^{54}(\gamma,n)Fe^{53}$ reaction. L. Katz and A. G. W. Cameron, Can. J. Phys. **29**, 518 (1951); R. Montalbetti, L. Katz, and J. Goldenberg, Phys. Rev. **91**, 659 (1953); J. H. Carver and K. H. Lokan, Australian J. Phys. **10**, 312 (1957).

²⁷ $Zn^{64}(\gamma,n)Zn^{63}$ reaction. L. Katz and A. G. W. Cameron, Can. J. Phys. **29**, 518 (1951).

and again detected the resultant positron activity with a thin window geiger counter. Katz's value is again higher than ours. This difference could be partly energy and partly activity calibration difference.

$Mo^{92}(\gamma,n)Mo^{91}$ (reference 28)

Our value for the $Mo^{92}(\gamma,n)Mo^{91}$ cross section refers to the (γ,n) reaction leaving the residual nucleus Mo^{91} in the ground state, and it is to be compared with Katz's σ_r . It is to be noted that Katz's results are based on an earlier decay scheme different from ours. His metastable state corresponds to the ground state in our decay scheme and no mixing is assumed to occur between the two states. Therefore, the cross section $\sigma(\gamma,n)$, determined in his experiment, should be lowered. We estimate that at 20.5 Mev it should be decreased to about 60 mb. This value is still higher than ours by about a factor of 2.

Recently, Mutsuro (1959) has remeasured the $Mo^{92}(\gamma,n)Mo^{91}$ cross section using a bremsstrahlung beam and detecting the resultant positron activity. His results, however, show a different curve shape and so the differences may be caused by curve analysis, energy calibration, and/or intensity calibration.

$Sb^{121}(\gamma,n)Sb^{120}$ (reference 29)

There exists a metastable state for Sb^{120} with a half-life $T_i=5.8$ days, much longer than the half-life T_g of the ground state ($T_g=16$ min). Therefore, by a proper choice of the activation time, the cross section for the (γ,n) reactions to the ground and to the metastable state can be separately determined. This was done by Katz and Cameron using a bremsstrahlung beam and detecting the resultant positron activity with a thin

²⁸ $Mo^{92}(\gamma,n)Mo^{91}$ reaction. L. Katz, Can. J. Phys. **31**, 250 (1953); N. Mutsuro, Y. Ohnuki, K. Sato, and M. Kimura, J. Phys. Soc. Japan **14**, 1649 (1959).

²⁹ $Sb^{121}(\gamma,n)Sb^{120}$ reaction. L. Katz and A. G. W. Cameron, Can. J. Phys. **29**, 518 (1951).

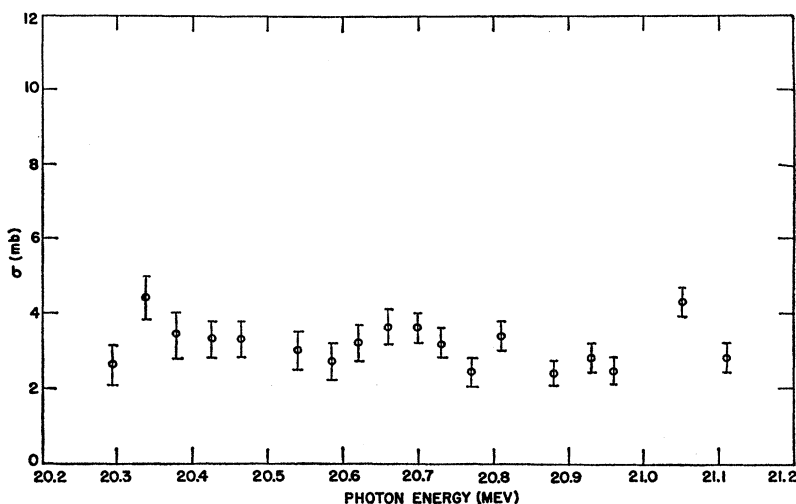


FIG. 7. The $F^{19}(\gamma,n)F^{18}$ reaction cross section in millibarns as a function of photon energy in Mev.

window geiger counter. Their measurements, which extend up to 18 Mev, do not overlap with ours, and therefore do not allow a direct comparison. However, our small value for the cross section $\sigma_g(\gamma,n)$, at 20.5 Mev, is not inconsistent with an extrapolation of Katz's curve and seems to indicate the absence of an appreciable tail at higher energies.

$Pr^{141}(\gamma,n)Pr^{140}$ (reference 30)

Various measurements of the (γ,n) cross section for Pr^{141} have all utilized bremsstrahlung beams. Carver and Turchinez detected the positron activity with the annihilation radiations and give a value of 80 mb at 20.5 Mev. Ferrero and co-workers similarly measured 75 mb, also greater than our value of 51.7 ± 5.5 mb. An analysis of Katz's neutron yield curve using the (γ,n) to $(\gamma,2n)$ ratio measured by Ferrero and Carver would give 37 mb at 20.5 Mev with considerable uncertainty.

In conclusion, we must say that the experimental situation for the (γ,n) cross section is still somewhat confused. When betatron results are compared it is found that the cross-section curves show large variations in absolute value and energy dependence. This experiment with monochromatic photons indicates agreement with some cross-section curves and suggests some of the major causes of error in others. Among the many factors which may affect betatron results, the primary ones seem to be energy calibration (above 19 Mev), lack of resolution in the yield curve, increasing uncertainty in analysis past the giant resonance, and errors in calibration of detectors.

As far as the accuracy of this experiment is concerned, we believe that the photon monitor and positron

detector were calibrated with a combined error which we estimate to be less than 4.5%. The Cu^{63} and Zn^{64} cross sections are limited by this error, but in the other cases counting statistics limited the accuracy. Fe^{54} and Cr^{50} also have considerable uncertainty in the level scheme.

B. Fine Structure

$C^{12}(\gamma,n)C^{11}$ Reaction

No obvious evidence of fine structure of the type reported from other experiments on carbon can be seen in our (γ,n) activation curve of C^{12} . There is, however, other experimental evidence of levels in C^{12} in the 20- to 21-Mev region. Katz³¹ has reported abrupt changes in slope in the neutron yield curve at 20.13, 20.29, 20.62, 20.90, and 21.08 Mev. The $C^{12}(\gamma,n)B^{11}$ experiment of Cohen *et al.*³² shows a level at about 20.8 Mev with a width of about 300 kev. Carroll and Stephens² total absorption experiment using monochromatic gamma rays indicates resonances at 20.15, 20.46, and 20.92 Mev of widths 165, 145, and 300 kev and integrated cross sections 1.6, 1.0, and 1.2 Mev-mb, respectively. In the present experiment, the resolution was measured to be of the order of 50-60 kev and the sensitivity was calculated to be about 0.1 Mev-mb. This should be more than adequate to detect resonances of the type reported. Therefore, a possible conclusion is that the energy resolution in this experiment was not as good as claimed, despite the fact that great care was taken in measuring the thickness of the tritium targets and in replacing them after a fixed irradiation time to avoid deposition of carbon onto the target. However, it is also possible that, in this energy region, overlapping of levels makes the experimental isolation of resonances difficult and that any sharp resonances in this region

³⁰ $Pr^{141}(\gamma,n)Pr^{140}$ reaction. F. Ferrero, R. Malvano, E. Silva, J. Goldemberg, and G. Moscati, *Nuclear Phys.* **10**, 423 (1959); J. H. Carver and W. Turchinets, *Proc. Phys. Soc. (London)* **73**, 110 (1959); L. Katz and G. Chidley, in *Nuclear Reactions at Low and Medium Energies* (Academy of Science, U.S.S.R., 1958).

³¹ L. Katz, National Bureau Standards, Photonuclear Conference, 1958 (unpublished).

³² L. Cohen, A. K. Mann, B. J. Patton, K. Reibel, W. E. Stephens, and E. J. Winhold, *Phys. Rev.* **104**, 108 (1956).

have integrated cross sections less than 0.1 Mev-mb. It must also be pointed out that no evidence for resolved resonances is found in the inverse reaction $B^{11}(\rho,\gamma_0)C^{12}$.³³ While this is inverse to $C^{12}(\gamma,\rho)$, the mirror nuclei C^{11} and B^{11} should be similar enough to make (γ,ρ) and (γ,n) similar. Consequently, the question of discrete resonances in the energy regions investigated is still unclear.

$F^{19}(\gamma,n)F^{18}$ Reaction

Although no experiments have been performed to determine the existence of levels in F^{19} in the energy region 20 to 21 Mev, Taylor and Goldemberg³⁴ reported

³³ D. Gemmel and H. Morton, Comptes Rendus du Congrès International de Physique Nucléaire; Interactions Nucléaires and Basses Energies et Structure des Noyaux, Paris, July, 1958 (Dunod, Paris, 1959), p. 694.

³⁴ J. Goldemberg and L. Katz, Phys. Rev. **95**, 471 (1954); J. G. V. Taylor, L. B. Robinson, and R. N. H. Haslam, Can. J. Phys.

evidence of "breaks" in the activation curve of the (γ,n) reaction in the energy region from threshold up to 17 Mev. Figure 7 shows $F^{19}(\gamma,n)F^{18}$ cross section between 20.2 and 21.1 Mev. The points seem to fluctuate, but this may be due, in part, to the carbon correction that amounts to 10-50% of the total cross section and enhances uncertainties in the curve. Since the sensitivity in the present measurement was of the order of 0.2 Mev-mb and the energy resolution between 50 and 60 kev, it is possible to set limits on size and frequency of level structure in this energy region; that is, the integrated cross section for resonances with a spacing larger than our energy resolution would have to be smaller than 0.2 Mev-mb or the level spacing would have to be comparable with our resolution or with the level widths. However, it is to be noted that the previous reservations about energy resolution are also pertinent to fluorine.

³², 238 (1954); W. L. Bendel, J. McElhinney, and R. A. Tobin, Phys. Rev. **111**, 1297 (1958).